SF_6 LEAK DETECTION USING TEA-CO_2 DIAL FOR HIGH VOLTAGE INSTALLATIONS

Parviz Parvin [1,2], Hasan Kariminezhad[1] , Fazel.Borna[3], Gholam-Reza Davoud-Abadi[1], Batool Sajad[4]

[1]Physics Department, Amirkabir university: P.O. Box 15875-4413,Tehran, Iran,Email: parvin@aut.ac.ir
[2]Laser Research center, Atomic Energy Organization of Iran, P.O. Box 11365-8486, Tehran, Iran
[3] Shahid Motahari center, Mashhad, Iran *[4] Physics Department, Azzahra university, Tehran, Iran*

ABSTRACT:

SF_6 with high dielectric strength is used in sealed HV installations to compact the electrical distribution sites. Therefore, the SF_6 leakage sensing has the environmental and economical significance. Here we have quantitatively shown that DIAL using a pair of pulsed CO_2 lasers enables us to detect SF_6 effluent in ppm level at relatively longer distances respect to competitive CW laser based BAGI[1] and passive IMSS[2] systems. Moreover, investigating temporal distribution of SF_6 emission from DIAL response indicates that heavy SF_6 molecules are reluctant to diffuse fast, willing to accumulate over the ground at definite locations.

1. INTRODUCTION:

Sulfur hexafluoride has a remarkable dielectric strength. Because of this natural property, it has been used as insulating gas in most of high-voltage equipments. In principle, SF_6 is widely used as an insulator in electrical installations particularly in high voltage circuit breakers and switch gears. Moreover it is used as insulator in compact HV distribution installation. This gas is an ideal dielectric, but although it is chemically inert to be a contributor to the greenhouse effect.

Because SF_6 is colorless, the leak sensing has traditionally relied on soap bubble or sniffer testing to locate SF_6 leakage. This involves de-energizing the equipment, and spraying liquid soap on it so that gas leaks create bubbles. Sniffers are gas detection units that vacuum air samples from equipment to detect the SF_6 presence. Both techniques require the leak inspector to be in close approximity to the equipment, which often means excessive climbing and reaching if the equipment is off the ground. In addition to being labor-intensive, soap bubble and sniffer testing are time-consuming and costly[2].

Another way to detect leaking gas is to use a known photo-acoustic effect. The incident light is absorbed by the gas at certain wavelength leading to heat the gas. When the heated gas expands, it produces pressure and acoustic waves to propagate from the point of heating. If the absorbed energy is sufficient, then the sound is detected by a microphone.

However, emerging optical imaging technologies provide a tool to identify quickly high probable leaking components. Remote sensing and instantaneous detection capabilities of those optical imaging technologies allow an inspector to scan quickly large areas containing numerous potential leaks. Optical imaging is currently used to identify SF_6 leaks at power facilities and has also shown great promise for fugitive emissions control at refineries and chemical plants. An important research step is currently being to develop instruments to quantify the mass emission rate of detected leaks.

The passive technique, Image Multi-Spectral Sensing (IMSS) is based on diffractive optics principle. It is a combination of a diffractive imaging spectrometer and an adaptive tunable filter. A conceivable instrument might consist of an ordinary IR-imaging radiometer whose detector is filtered to respond only to light at the wavelength absorbed by the gas to be detected. Plume imaging would be accomplished by cloud attenuation of thermal radiation rather than scattered sunlight. Unfortunately, the amount of radiation that is emitted within the absorption bandwidth of the gas of interest is so small to characterize very low signal-to-noise ratios[2].

On the other hands, the active imaging system, Backscatter Absorption Gas Imaging (BAGI) employs a CW CO_2 laser. The tunability of the CO_2 laser over about 60 usable vib-rotational lines in the 9 to 11μm makes it possible to image many gases, not only SF_6 at 10.55 μm but also hydrocarbon gases such as propan (C_3H_8) and pentan (C_5H_{12}) at 10.81μm and 9.67μm , respectively and many other gas components mostly produced in oil refinery and petrochemical plants. The ideal IR source is one that is peaked at the maximum absorption wavelength of the gas and has an infinitely narrow bandwidth to attain maximum gas-cloud contrast. The laser must be intensive enough to produce backscatter light that is indeed significantly higher than that of the passive emission into IMSS.

Gas imaging occurs when a gas absorbs the laser light within the laser-illuminated field of view, thereby attenuating the backscattered laser light and producing a darkened region in the TV display whenever the gas is present. The higher the gas concentration, the greater

the absorption to produce better contrast. In this manner, the invisible gas becomes visible on the video and its origin, size and direction of movement are easily determined. In the absence of an absorbing gas, the energy reflected from backscattered laser component produces an image of the terrain at the monitor. When the absorbing gas is present, both the incoming and backscattered laser radiation are reduced due to the strong molecular absorption of the gas at the laser wavelength. The difference in contrast between the area and the environment produces an image or shadow of the gas cloud on the monitor [1].

Most laser systems that use topographic targets incorporate either pulsed or CW laser with direct or heterodyne detection primarily to achieve long measurement ranges. Continuous-wave systems using direct detection are known as remote sensors of toxic and hazardous gases at relatively short distances. Pulsed CO_2 laser has been shown to be a useful probe for concentration, temperature, pressure and the velocity of molecular constituents in the atmosphere [3].

In this work, we empirically show that DIAL, regarding the CW laser based BAGI, is an appropriate technique to locate SF_6 leakage as well as to evaluate its mass rate emission.

2. THEORY:

The BAGI backscattered laser power incident upon the detector (P_S) is given by[1]

$$P_S = P_0 \Omega \beta \eta_{TL} \eta_{RL} e^{-2\int_0^R K(\lambda_L, R)dR} \quad (1)$$

where η_{TL} is the efficiency of the beam-transmission optics at the laser wavelength λ_L and exponential statement is the baseline atmospheric transmission at the laser wavelength. $\Omega=A_0/R^2$ is the system collection solid angle. η_{RL} represents the optical transfer efficiency of the synchroscan collection optics. P_0 is the output laser power and β represent the bidirectional reflectance function.

The elastic scattering form of lidar equation is [4,5]

$$P_S = P_0 \frac{A_0}{R^2} \beta(\lambda_L, R) \frac{c\tau_L}{2} \xi(R) \xi(\lambda_L, R) e^{-2\int_0^R K(\lambda_L, R)dR} \quad (2)$$

Where, $\xi(R)$ and $\xi(\lambda_L,R)$ represent the overlap factor and the receiver's spectral transmission factor, respectively. $c\tau_L/2$ represents the lidar spatial resolution power and $\beta(\lambda_L,R)$ is the volume backscattering coefficient. $\kappa(\lambda_L,R)$ which is the attenuation coefficient

$$\kappa(\lambda_L, R) = \bar{\kappa}(\lambda_L, R) + N\sigma_{abs}(\lambda_L) \quad (3)$$

is exclusive of absorption and scattering contributions from the molecular species and the background.

DIAL lidar equation is shown as:

$$\frac{P(\lambda_{on}, R)}{P(\lambda_{off}, R)} = \frac{\xi(\lambda_{on})\beta(\lambda_{on}, R)}{\xi(\lambda_{off})\beta(\lambda_{off}, R)} e^{-2\int_0^R \{\kappa(\lambda_{on}, R) - \kappa(\lambda_{off}, R)\} dR} \quad (4)$$

The absorbing line (λ_{on}) is on the strong absorption peak of interest molecule and the λ_{off} is off the peak. λ_{on} and λ_{off} should be close enough (as it is in most of atoms) to presume the same $\beta(\lambda_L,R)$ which is not the case for larger absorption bandwidth in SF_6 molecules. However, for simplicity, the effect of $\beta(\lambda_L,R)$ in Eq. 4 is assumed to be negligible. Therefore, we neglect the effect of the second term appears in Eq.5 to rewrite the local concentration, as given by:

$$N(R) \approx \frac{1}{2\sigma_A(\lambda_{on} : \lambda_{off})} [\frac{d}{dR} (\ln \frac{P_s(\lambda_{off}, R)}{P_s(\lambda_{on}, R)})] \quad (5)$$

where, the laser lines are selected to be λ_{on} =10.551μm and λ_{off} =10.247μm for our experiments. It states that gaseous concentration is proportional to the derivative logarithm of signal ratio at λ_{on} and λ_{off}. Therefore, it is proportional to the slope of DIAL $\ln P_S$–R response.

Consequently, we obtain the linear relationship given by

$$S = 2\sigma_A(\lambda_{on} : \lambda_{off}) N(R) + S_0 \quad (6)$$

where $S=d/dR[\ln P(\lambda_{on}, R)]$ and $S_0=d/dR\ [\ln P(\lambda_{off},R)]$. S_0 is the abscissa and $2\sigma_A(\lambda_{on}:\lambda_{off})= 2[\sigma_{abs}(\lambda_{on}) - \sigma_{abs}(\lambda_{off})]$ denotes the slope of the straight line.

The effect of topographic surface is significant on the signal received by the detector. For example, in image processing using a typical MCT detector the corresponding received backscattered signals are listed in table.1 at the presence or the absence of topographic surface. The detector is located ~ 700m far from the gas leakage. It indicates that the signal power backscattered from the installation walls is ~ seven order of magnitude greater.

Table.1 DIAL backscattered signals (a) from a topographic target and (b) at the absence of that target

Range	Telescope Dia.	P_S (a)	P_S (b)
700m	0.5m	2.23mW	0.27nW

3. EXPERIMENT SET-UP:

A home-assembled DIAL was implemented in Shahid Motahari center to study the optical sensing of the SF_6 gas, released into atmosphere. DIAL is equipped with a pair of tunable TEA - CO_2 laser having 0.3 Hz pulse repetition rate, 200 nsec FWHM with 200 μsec time delay between the subsequent pulses at tuned λ_{on} and

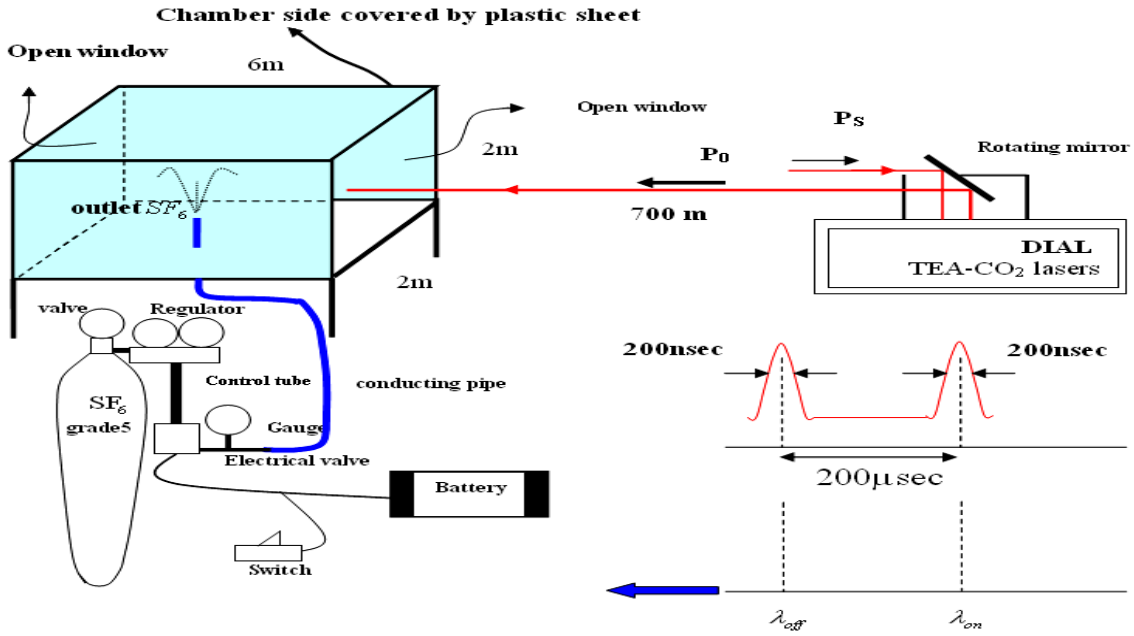

Fig. 1. Experimental scheme of SF_6 discharge into atmosphere.

detuned λ_{off} . A gas mixture of $(CO_2{:}He{:}N_2) \approx (2{:}5{:}1)$ was filled in the tube at 0.6 atmospheric pressure. The laser is tunable over approximately 60 lines within the R and P branches of the CO_2 laser transitions. A 5×5 cm^2 Littrow grating with 40 grooves/mm was used as the dispersive element situated in the laser resonator to deliver a bandwidth of $0.5cm^{-1}$ at 10.6 μm laser line. A Cassegrain telescope receives the FIR photons to focus those photons at a $1\times1mm^2$ N_2-cooled MCT (HgCdTe) detector to decrease optimally the environmental noises. The amplified received signals are collected through A/D converter during a collection period of ~ 20nsec to plot the signal-range graph.

4. RESULTS AND DISCUSSION:

In order to evaluate the DIAL ability for SF_6 leak detection, a discharge experiment, including a $2m\times2m\times6m$ irradiation cell was arranged as shown in fig.1. At first, a cylindrical tube with 5mm diameter and 1m length was filled with SF_6 at various 3-10 bar constant pressures. DIAL, at 10.551μm sends the laser shots to the irradiation cell which is located 700m afar, just at the end of SF_6 discharge process into the cell. Table.2 illustrates the amount of SF_6 released into the cell at various tube pressures. It indicates that a SF_6 amount as minimum as 2.2 ppm, can be detected by DIAL.

A typical P_S-R plot of DIAL is illustrated in fig.2, to show that a drastic change appears at the discharge location. The slopes due to the corresponding lines give us the concentration N(R) quantitatively. Assuming SF_6 to be an ideal gas at those pressures, the Bernoullie approximation is written in Eq.7

$$\frac{1}{2}\rho_i v_i^2 + \rho_i g h_i + P_i = \frac{1}{2}\rho_f v_f^2 + \rho_f g h_f + P_f = cte \qquad (7)$$

Mass conservation law is used to obtain concentration in ppm as terms of the initial tube pressure (P_0) and the discharge time (t).

$$Concentration(ppm) = 16.224t\sqrt{P_i} \qquad (8)$$

Moreover, SF_6 has two major isotopes, $^{32}SF_6$ and $^{34}SF_6$ with %96 and %4 abundances, respectively. The absorption spectrum of SF_6 denotes the peaks due to both isotopes to be at $948cm^{-1}$ and 931 cm^{-1}, respectively.

Another experiment was carried out at various initial SF_6 Pressure for 2sec constant discharge time. The calculated concentration can be given in terms of the initial SF_6 pressures. Fig.3 depicts the SF_6 DIAL slope versus SF_6 concentration which is a linear relationship. It is in agreement to Eq.6. Neglecting the multi-photon absorption process and assuming the single photon absorption with an equivalent cross-section in order of $10^{-20}cm^{-2}$, the linearity according to fig.3 is statistically derived, using the least square method, as below:

$$S = 4\times10^{-20}\,N + 0.007 \qquad (9)$$

The abscissa S_0=0.007 is the slope component due to λ_{off}. The linearity approves the negligible effect of β to derive Eq.5.

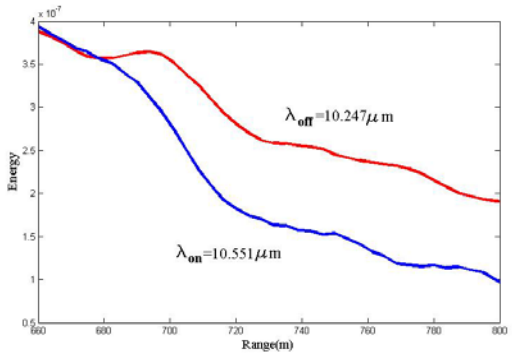

Fig. 2. P_S-R response of DIAL, comparing λ_{on} and λ_{off} graphs.

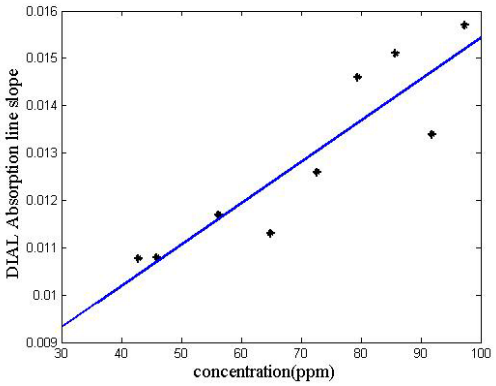

Fig. 3. DIAL slope versus SF_6 concentration.

Table.2 SF_6 released into the cell at various pressures.

pressure (bar)	3	4	7	10
Concentration (ppm)	2.2	2.9	5.0	7.4

We have analyzed numerous data of DIAL using the concentration criteria based on the logarithmic derivative of the signal ratios at λ_{on} and λ_{off} , to determine the local concentration versus distance. Fig.4 shows that SF_6 gas slowly diffuses through atmosphere according to the following one dimensional diffusion equation:

$$\frac{\partial N}{\partial t} + U\frac{\partial N}{\partial x} = \frac{\partial^2 \varepsilon_x N}{\partial x^2} \qquad (10)$$

Where N is the concentration, ε_x denotes the diffusivity constant and U represents the x-direction wind velocity. The gaussian diffusion FWHM was broadened ~ 50m around the location of the SF_6 fugitive emission during ~ 10sec, after the end of the gas discharge.

DIAL data are collected assuming still weather without the consideration of the wind or the rain. In general, the metrological parameters as well as topology of area become significant during the SF_6 diffusion.

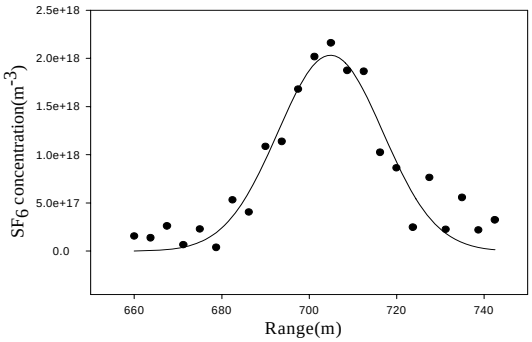

Fig. 4. A typical Gaussian diffusion of SF_6 in the static atmosphere 10sec after the discharge.

5. CONCLUSION:

In this work, the remote sensing of the green house gas SF_6 is experimentally studied. According to green house effect, it is necessary to make an effort to minimize SF_6 leakage into the atmosphere using more sensitive optical monitoring systems.

It is shown, here, that a compact DIAL, using TEA-CO_2 laser could be an efficient alternative for the CW CO_2 laser based BAGI to asses mass emission rate of SF_6 effluent. It is applied mainly in HV installation without any need for topographic targets. The SF_6 amount, in ppm level, was successfully detected where the gas is released into atmosphere ~ 700m far from the detector. Analyzing data, we have shown that the SF_6 accumulation is significant, because of its sluggish diffusion over the ground due to its relative small diffusivity constant.

6. REFERENCES:

1. McRae T.G and Kulp T.J., Backscatter absorption gas imaging: a new technique for gas visualization, *Applied Optics*, Vol.32. No.21, 1993.

2. Robinson D.R and Luke-Boon R.E, Identifying Fugitive Emissions with optical Imaging,*23th international petroleum environmental conference*.

3. Carlisle .C.B, et al, CO2 laser-based differential absorption lidar system for range-resolved and long-range detection of chemical vapor plumes, *Apllied optics*,Vol.34, No.27, 1995.

4. Parvin .P and Kariminezhad .H, *Iranian Patent*, No.38405038, 2005.

5. Parvin .P, et al, The remote sensing of radioactive plumes with a hybrid system including gamma spectroscopy and dial lidar, *22th ILRC*, Matera, Italy, 2004.